The BRAAFF checklist: a new dermoscopic algorithm for diagnosing acral melanoma

A. Lallas,[1] A. Kyrgidis,[1] H. Koga,[2] E. Moscarella,[1] P. Tschandl,[3] Z. Apalla,[4] A. Di Stefani,[5] D. Ioannides,[2] H. Kittler,[4] K. Kobayashi,[6,7] E. Lazaridou,[2] C. Longo,[1] A. Phan,[8] T. Saida,[3] M. Tanaka,[6] L. Thomas,[8] I. Zalaudek[9] and G. Argenziano[10]

[1]Skin Cancer Unit, *Arcispedale Santa Maria Nuova IRCCS, Viale Risorgimento 80, 42100 Reggio Emilia, Italy*
[2]Department of Dermatology, *Shinshu University School of Medicine, Matsumoto, Japan*
[3]Division of General Dermatology, *Department of Dermatology, Medical University, Vienna, Austria*
[4]First Department of Dermatology, *Medical School, Aristotle University, Thessaloniki, Greece*
[5]Division of Dermatology, *Complesso Integrato Columbus, Rome, Italy*
[6]Department of Dermatology, *Tokyo Women's Medical University Medical Center East, Tokyo, Japan*
[7]*Kobayashi Clinic, Tokyo, Japan*
[8]Department of Dermatology, *Claude Bernard – Lyon 1 University, Centre Hospitalier Lyon-Sud, Pierre Bénite, France*
[9]Department of Dermatology and *Venereology, Medical University, Graz, Austria*
[10]Dermatology Unit, *Second University of Naples, Naples, Italy*

Correspondence
Aimilios Lallas.
E-mail: emlallas@gmail.com

Accepted for publication
7 July 2015

Funding sources
This study was supported in part by the Italian Ministry of Health (RF-2010-2316524).

Conflicts of interest
None declared.

Summary

Background The parallel ridge pattern (PRP) is considered the dermoscopic hallmark of acral melanoma (AM). However, it was recently shown that approximately one-third of AMs do not display a PRP dermoscopically, rendering their detection more troublesome.
Objectives To investigate the diagnostic accuracy of dermoscopic criteria for the diagnosis of AM.
Methods Dermoscopic images of consecutive cases of histopathologically diagnosed AMs and acral naevi with histopathological diagnosis or with at least 1 year of follow-up were evaluated by three independent investigators for the presence of predefined criteria. Crude and adjusted odds ratios and their corresponding 95% confidence intervals were calculated by univariate and multivariate logistic regression, respectively. Receiver operating characteristic curves were used to choose among competing classification schemes.
Results In total 603 lesions (472 naevi and 131 AMs) were included in the study. A scoring system (named BRAAFF) composed of six variables was associated with optimal area under the curve and sensitivity for the diagnosis of AM. This method includes four positive (irregular blotches, ridge pattern, asymmetry of structures and asymmetry of colours) and two negative predictors (furrow pattern and fibrillar pattern).
Conclusions The BRAAFF checklist significantly improves the diagnostic accuracy of dermoscopy for the diagnosis of AM.

What's already known about this topic?

- Approximately one-third of acral melanomas (AMs) lack a dermoscopic parallel ridge pattern, rendering their detection more troublesome.

What does this study add?

- A scoring system composed of six variables achieves the highest diagnostic accuracy for AM.
- Application of this diagnostic scheme minimizes the possibility of missing AMs that are not dermoscopically characterized by a parallel ridge pattern.

Acral melanoma (AM) represents the most common melanoma subtype in nonwhite populations, accounting for > 70% of melanomas in African Americans and approximately 50% of melanomas in Asian patients.[1–6] In white patients, melanoma develops most often in nonacral sites, with AM accounting for < 10% of cases.[7,8] However, these differences are rather related to the prevalence of nonacral melanoma in white populations, as the absolute incidence of AM has been estimated to be similar among all ehtnicities.[7–9] Of note, AM has been associated with a worse prognosis compared with other melanoma subtypes. As no pathophysiological mechanism has been suggested to explain its particularly unfavourable clinical course, it has been attributed mainly to a delayed diagnosis.[10–12]

Early detection is the only safe strategy to reduce melanoma-related mortality, as, irrespectively of the tumour site, the prognosis of the disease depends directly on the invasion depth at the time of diagnosis. Dermoscopy has been shown optimally to serve the goal of early diagnosis, by enabling clinicians to recognize melanoma before it develops macroscopically evident characteristics.[13] In acral pigmented lesions, dermoscopy enhances melanoma recognition by highlighting the accentuation of the pigmentation on the skin ridges [parallel ridge pattern (PRP), in contrast to the parallel furrow pattern (PFP) of acral naevi].[9,14–28] However, it has recently been shown that approximately one-third of AMs do not display a PRP, thus rendering their accurate diagnosis more difficult.[29] Some additional features, such as irregular diffuse pigmentation and other nonsite-specific melanoma criteria, have also been reported to characterize AM.[15–18,25,27]

The aim of the present study was to develop and validate a multivariable dermoscopic prediction model for the differentiation between early AMs and acral naevi.

Materials and methods

This was a multicentre morphological study conducted in seven specialized centres for skin cancer diagnosis and management in Austria, France, Greece, Japan and Italy. The databases of our centres were screened to identify eligible cases. Eligibility criteria were the histopathological diagnosis of AM or acral naevus, or the clinicodermoscopic diagnosis of acral naevus with available follow-up of at least 1 year, as well as the availability of high-quality dermoscopic images. First we searched for cases of histopathologically diagnosed AMs or acral naevi fulfilling the inclusion criteria. Then we added to the study sample consecutive cases of nonexcised acral naevi with at least 1 year of follow-up, in order to reach a number comparable with the other two groups. Nail-apparatus melanomas without involvement of the acral skin were excluded from the study. Patients' data were recorded, including age, sex, location (palm or sole) and Breslow thickness.

Upon inclusion and prior to dermoscopic evaluation, patients were randomly allocated to either a training or a validation dataset. However, because of the limited sample size and the need to include many predictors, we finally elected to include all patients in a single dataset, increasing the ratio of cases to independent variables, in order to include more variables in the final model and obtain the highest possible sensitivity. The training and validation sets were analysed separately for the purpose of sensitivity analyses. The registry data from the seven skin cancer centres were used for both the development and the validation, using resampling and splitting of the original dataset.

Dermoscopic evaluation

Dermoscopic images were evaluated by three independent investigators (H. Koga, E.M., P.T.), blinded for the histopathological and clinicodermoscopic diagnoses. The investigators were asked to assess the global dermoscopic pattern of each lesion, as well as the presence or absence of predefined dermoscopic structures. The selection of the dermoscopic criteria was based on the available literature and was a result of consensus among the authors.[14–27] The dermoscopic variables used are analytically described in Table 1. Of 15 dermoscopic variables included in the analysis, 14 were dichotomous, and the global pattern was categorical with six different values.

Statistical analysis

Intraobserver agreement was examined with Cohen's kappa and the intraclass correlation coefficient (ICC). The outcome to be predicted by the prediction model was a dichotomous variable with the final diagnosis, as determined either by histopathological examination or by 1 year of follow-up (0, acral naevi, both excised and nonexcised; 1, AM). All separate dermoscopic variables were included in the analysis and examined as possible predictors of AM. As the evaluators blindly assessed all included lesions, a complete-case analysis was feasible.

In order to have sufficient power for a prediction model, at least 10 events per degree of freedom (each beta) spend is needed. The final combined set included 131 melanomas, indicating that the sample size is small given the number of predic-

Table 1 Definitions of dermoscopic criteria

Dermoscopic variable	Definition
Global pattern	
Parallel lines	The pigmentation follows a pattern of parallel lines, either following the skin markings (sulci or cristae) or not
Reticular	A pigment network covering the major part of the lesion
Globular	Numerous variously sized, round-to-oval structures with various shades of brown and grey-black coloration
Structureless	A diffuse coloration without any identifiable structures
Starburst	Pigmented streaks arranged radially at the edge of the lesion
Multicomponent	A combination of two or more different patterns, clearly present in a given lesion
Asymmetry of structures	Identifiable structures are not symmetrically distributed all over the lesion
Asymmetry of colours	Identifiable colours are not symmetrically distributed all over the lesion
Parallel ridge pattern	Parallel pigmented lines following the cristae of the glabrous skin
Parallel furrow pattern	Parallel pigmented lines following the sulci of the glabrous skin
Fibrillar pattern	Numerous, finely pigmented filaments perpendicular to the furrows and ridges
Lattice-like pattern	Pigmentation following and crossing the furrows
Irregular blotches	Black, brown and/or grey structureless areas with asymmetric distribution within the lesion
Irregular dots/globules	Black, brown, round-to-oval, variously sized structures irregularly distributed within the lesion
Irregular streaks/pseudopods	Bulbous and often kinked or finger-like projections asymmetrically distributed at the periphery of a lesion
Blue-white veil	Irregular, structureless area of confluent blue pigmentation with an overlying white 'ground-glass' film. The pigmentation cannot occupy the entire lesion and usually corresponds to a clinically elevated part of the lesion
Regression structures	White scar-like depigmentation and/or blue pepper-like granules usually corresponding to a clinically flat part of the lesion
Atypical vessels	The presence of more than one morphological type of vessel or the presence of linear irregular vessels, or the presence of other types of vessels with an irregular distribution
Atypical network	Black, brown or grey network with irregular holes and thick lines
Milky-red areas	Areas of structureless pink colour within the lesion

tors selected for regression modelling. This limitation is discussed further below.[30] Accordingly, we selected not to use the training set, but to develop the model from the complete dataset. This also imposes some limitations, as discussed below.

Colinearity was assessed via a correlation matrix, using Spearman's rho correlation coefficient. Relative risks were calculated for all dichotomous variables. Crude odds ratios (ORs), adjusted ORs and the corresponding 95% confidence intervals (CIs) were calculated by univariate and conditional multivariate logistic regression, respectively. Conditional backward elimination proved more parsimonious.

To assess the internal validity and degree of overoptimism (calibration) in the models, the bootstrap resampling technique was applied by fitting the logistic model in a bootstrap sample of 400 subjects drawn from the original sample over 100 repetitions. The averaged difference in performance as a stable estimate of the optimism was subtracted from the apparent performance to estimate the internally validated performance.[31]

The alpha level was set at 0·05, while an alpha level of 0·10 was used as cut-off for variable removal in the automated model selection for multivariate logistic regression. For logistic regression analyses, we created an 'intrarater' set of variables in which an agreement between at least two raters was required to confirm any specific value. In those cases where this was not possible, the value was chosen upon re-evaluation of the images and consensus.

Discriminant analysis was performed and functions were saved; we then used receiver operating characteristic (ROC) curves to choose between competing classification schemes. Specificity and sensitivity were extracted from classification tables. The type I error probability associated with all tests in this study was set to 0·05. All statistical calculations were made with SPSS 17.0 (IBM, Armonk, NY, U.S.A.).

Results

In total 603 lesions from 603 patients were included in the study; 472 were naevi (183 excised and 289 not excised) and 131 were melanomas (42 *in situ* and 89 invasive tumours). The inclusion period was from the beginning of 2010 to the end of 2013. The mean Breslow thickness of invasive AMs was 2·67 mm (range 0·2–14·5). The mean age of the whole study group was 42·3 years (range 1–98). The mean age of patients with melanoma was significantly higher (67·7 years, with the youngest patient aged 21 years) than that of patients in the naevi group (35·6 years). Age was found to be associated with a 9·5% increased risk for melanoma per year of age added, in an adjusted model with all dermoscopic variables included (adjusted OR 1·10, 95% CI 1·07–1·12, $P < 0·001$). The male-to-female ratio was 1 : 1·6 and did not differ significantly between patients with AM and acral naevi. The majority of the lesions were located on the sole (538 of 603, 89·2%), and only 65 (10·8%) were palmar. The anatomical site distribution (soles/palms) was similar for naevi and melanomas.

Detailed results of the dermoscopic analysis are given in Table 2. The global pattern of parallel lines was by far the most frequent in naevi (73·7%, Fig. 1) and in melanoma *in situ* (62%). In contrast, invasive melanoma most commonly

Table 2 Frequency of dermoscopic criteria in 603 acral lesions according to diagnosis

Dermoscopic variable	Naevus excised (n = 183)	Naevus not excised (n = 289)	Naevus total (n = 472)	Melanoma *in situ* (n = 42)	Melanoma invasive (n = 89)	Melanoma total (n = 131)
Global pattern						
Parallel lines	122 (66·7)	226 (78·2)	348 (73·7)	26 (62)	9 (10)	35 (26·7)
Reticular	4 (2·2)	5 (1·7)	9 (1·9)	2 (5)	0	2 (1·5)
Globular	6 (3·3)	17 (5·9)	23 (4·9)	2 (5)	1 (1)	3 (2·3)
Structureless	34 (18·6)	31 (10·7)	65 (13·8)	4 (10)	34 (38)	38 (29·0)
Starburst	0	1 (0·3)	1 (0·2)	0	0	0
Multicomponent	17 (9·3)	9 (3·1)	26 (5·5)	8 (19)	45 (51)	53 (40·5)
Asymmetry of structures	30 (16·4)	19 (6·6)	49 (10·4)	20 (48)	84 (94)	104 (79·4)
Asymmetry of colours	30 (16·4)	14 (4·8)	44 (9·3)	24 (57)	84 (94)	108 (82·4)
Parallel ridge pattern	4 (2·2)	5 (1·7)	9 (1·9)	21 (50)	29 (33)	50 (38·2)
Parallel furrow pattern	98 (53·6)	184 (63·7)	282 (59·7)	6 (14)	7 (8)	13 (9·9)
Fibrillar pattern	39 (21·3)	66 (22·8)	105 (22·2)	4 (10)	6 (7)	10 (7·6)
Lattice-like pattern	24 (13·1)	30 (10·4)	54 (11·4)	0	0	0
Irregular blotches	26 (14·2)	18 (6·2)	44 (9·3)	14 (33)	76 (85)	90 (68·7)
Irregular dots/globules	24 (13·1)	22 (7·6)	46 (9·7)	10 (24)	51 (57)	61 (46·6)
Irregular streaks/pseudopods	3 (1·6)	2 (0·7)	5 (1·1)	1 (2)	6 (7)	7 (5·3)
Blue-white veil	21 (11·5)	10 (3·5)	31 (6·6)	2 (5)	41 (46)	43 (32·8)
Regression structures	5 (2·7)	1 (0·3)	6 (1·3)	3 (7)	14 (16)	17 (13)
Atypical vessels	1 (0·5)	1 (0·3)	2 (0·4)	0	14 (16)	14 (10·7)
Atypical network	2 (1·1)	0	2 (0·4)	2 (5)	0	2 (1·5)
Milky-red areas	1 (0·5)	2 (0·7)	3 (0·6)	0	19 (21)	19 (14·5)

Values are n (%).

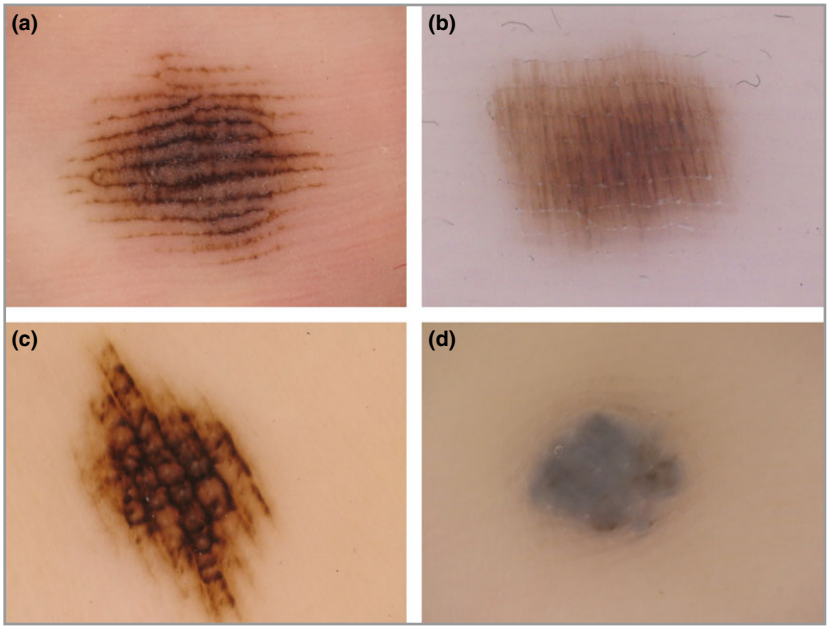

Fig 1. The most common global dermoscopic pattern of acral naevi was parallel lines – (a) parallel furrow pattern, (b) fibrillar pattern and (c) lattice-like pattern – followed by the structureless pattern (d).

exhibited a multicomponent (51%) or structureless pattern (38%, Fig. 2).

Intraobserver agreement

In all cases, Cohen's kappa ranged from 0·496 to 0·794, showing moderate (for a few variables including regression structures, irregular streaks/pseudopods and atypical network) to substantial agreement between raters. ICC (using averaged measures, absolute agreement) ranged from 0·526 to 0·828, showing moderate to good agreement among raters. Regression structures, irregular streaks/pseudopods and atypical network were the only variables with ICC < 0·679.

Univariate and multivariate analyses

The results of the univariate and multivariate analyses are shown in Tables 3 and 4, respectively. In the univariate

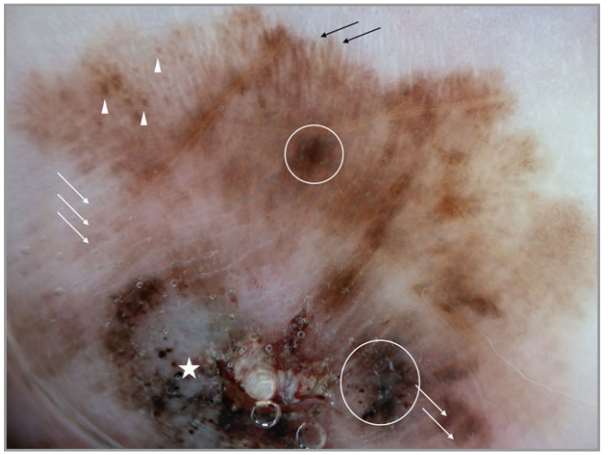

Fig 2. A 1·4-mm-thick melanoma displaying several criteria, including a parallel ridge pattern (white arrows), irregular blotches (circles), irregular dots/globules (arrowheads), irregular streaks (black arrows) and a blue-white veil (star).

Table 3 Dermoscopic predictors of acral melanoma (melanoma total vs. naevus total). Univariate logistic regression analysis

Dermoscopic variable	P-value	OR	95% CI
Global pattern			
Parallel lines		Reference	
Reticular	0·054	0·22	0·048–1·03
Globular	0·001	0·13	0·039–0·43
Structureless	0·009	0·59	0·39–0·87
Starburst	1	0	0
Multicomponent	0·003	2·04	1·28–3·26
Dermoscopic criteria			
Asymmetry of structures	< 0·001	2·12	1·51–2·98
Asymmetry of colours	< 0·001	2·46	1·73–3·49
Parallel ridge pattern	< 0·001	5·56	2·73–11·30
Parallel furrow pattern	< 0·001	0·046	0·026–0·080
Fibrillar pattern	< 0·001	0·095	0·050–0·18
Lattice-like pattern	1·00	0	0
Irregular blotches	< 0·001	2·05	1·43–2·93
Irregular dots/globules	0·15	1·33	0·90–1·94
Irregular streaks/ pseudopods	0·57	1·40	0·44–4·41
Blue-white veil	0·17	1·39	0·87–2·20
Regression structures	0·028	2·83	1·12–7·19
Atypical vessels	0·010	7·00	1·59–30·80
Atypical network	1	1·00	0·14–7·10
Milky-red areas	0·003	6·33	1·87–21·40

OR, odds ratio; CI, confidence interval. $P < 0·05$ is significant.

analysis, several variables showed statistically significant predictive value to differentiate melanoma from naevi (Table 3). However, in the multivariate analysis, a reduced number of variables remained important predictors, adjusted for the effect of the remainder variables (Table 4).

Based on the multivariate model, we employed discriminant analyses to test different scoring schemes and to determine the optimal cut-off thresholds. We ran a number of sensitivity analyses, using the training and the validation sets, along with the complete set. We opted for the highest possible sensitivity of the multivariate predictive model. Optimal area under the curve and sensitivity were our end points. We developed the following scoring system composed of six variables (blotches, ridge pattern, asymmetry of structures, asymmetry of colours, furrow pattern and fibrillar pattern), which was thus named BRAAFF (Table 5):

Score = irregular blotch + (3 × parallel ridge pattern) + asymmetry of structures + asymmetry of colours − parallel furrow pattern − fibrillar pattern.

A threshold of one point was found to provide the best sensitivity (93·1%), supplemented by satisfying specificity (86·7%), and allowing correct classification of 88·1% of the overall group cases (all melanomas vs. all naevi). The ROC curve is plotted in Figure 3. The model yielded a corrected area under the curve of 0·954 (95% CI 0·929–0·979, $P < 0·001$).

The frequencies of dermoscopic criteria within each group of patients are presented in Table 2. Furthermore, we employed sensitivity analyses to examine the diagnostic accu-

Table 4 Dermoscopic predictors of acral melanoma (melanoma total vs. naevus total). Multivariate logistic regression analysis

Dermoscopic variable	P-value	Adjusted OR	95% CI
Parallel ridge pattern	< 0·001	16·20	5·85–44·89
Asymmetry of colours	0·001	6·85	2·13–22·01
Irregular blotches	0·001	3·60	1·70–7·62
Asymmetry of structures	0·041	3·47	1·05–11·43
Fibrillar pattern	0·012	0·28	0·10–0·75
Parallel furrow pattern	< 0·001	0·12	0·054–0·28

Variables entered on model: global pattern (categorical, reference = parallel lines pattern), asymmetry of structures, asymmetry of colours, parallel ridge pattern, parallel furrow pattern, fibrillar pattern, lattice-like pattern, irregular blotches, irregular dots/globules, irregular streaks/pseudopods, blue-white veil, regression structures, atypical vessels, atypical network, milky-red areas. Odds ratio (OR) mutually adjusted for all variables in the model. Relative risks (RRs) approximated by ORs, 95% confidence intervals (CIs) and P-values were calculated with a conditional multivariate logistic regression conditional backward elimination model. RRs were mutually adjusted for variables in the model. Logit for all independent dichotomous variables = no. Alpha level set to $P < 0·05$. Cut-off value set to 0·10.

Table 5 The BRAAFF checklist for the diagnosis of acral melanoma

Acronym	Criterion	Points
B	Irregular **b**lotch	+ 1
R	Parallel **r**idge pattern	+ 3
A	**A**symmetry of structures	+ 1
A	**A**symmetry of colours	+ 1
F	Parallel **f**urrow pattern	− 1
F	**F**ibrillar pattern	− 1

A total score of ≥ 1 is needed for a diagnosis of melanoma.

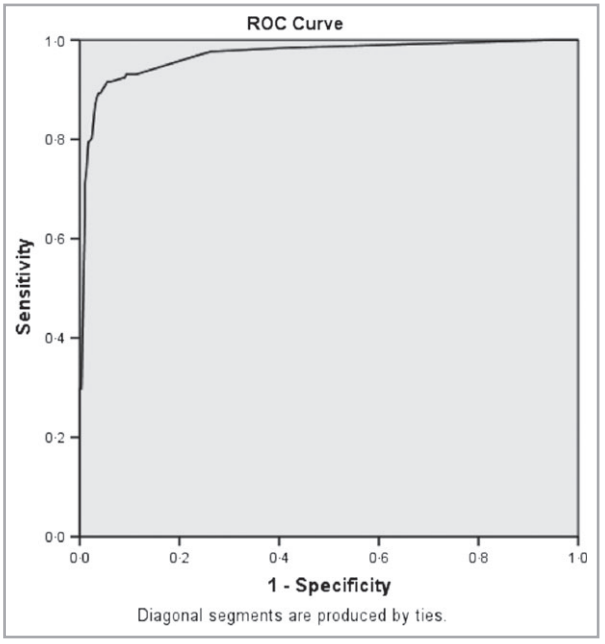

Fig 3. Receiver operator characteristic (ROC) curve. The model includes asymmetry of structures, asymmetry of colours, parallel ridge pattern, parallel furrow pattern, fibrillar pattern and irregular blotch, and yields a corrected area under the curve of 0·95 (95% confidence interval 0·93–0·98, $P < 0·001$).

Table 6 Assessment of the accuracy of the BRAAFF checklist for the diagnosis of acral melanoma in different subgroups of lesions

Subgroups	Sensitivity (%)	Specificity (%)
All melanomas vs. all naevi	93·1	86·7
Melanoma *in situ* vs. all naevi	81·0	89·6
Invasive melanoma vs. all naevi	96·6	92·6
All melanomas vs. excised naevi	89·3	86·9
All melanomas vs. nonexcised naevi	91·6	94·5

racy of our model in certain subgroups of patients. In detail, we assessed the accuracy of the model for the diagnosis of *in situ* and invasive melanoma. In addition, we tested the model when melanomas were compared only with excised naevi, which reasonably are morphologically less typical than the nonexcised ones. The results of the subgroup analysis are shown in Table 6.

Discussion

Our study confirms the high diagnostic accuracy of dermoscopy for the diagnosis of AM. Based on the results of our analysis, we propose a dermoscopic diagnostic algorithm that achieves 93·1% sensitivity and 86·7% specificity for melanoma diagnosis.

In line with pre-existing evidence on all melanoma subtypes, our study highlights that the age of the patient should always be considered when evaluating a pigmented skin lesion, as melanoma is extremely rare in children and its incidence increases with age.[32,33] The youngest patient in our series was aged 21 years, the mean age of patients with melanoma was significantly higher than that of patients in the naevi group, and every added year of age increased the risk of melanoma by 9·5%.

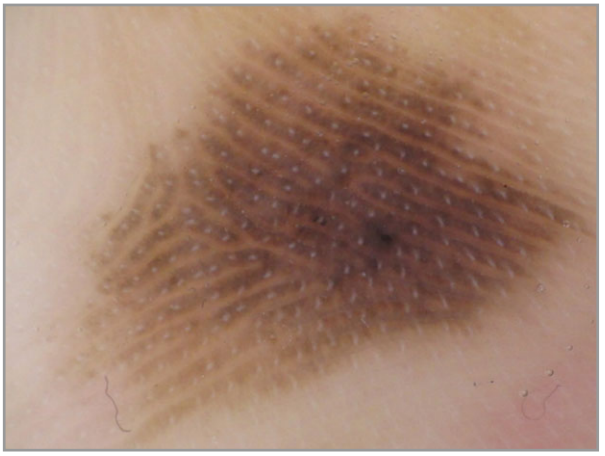

Fig 4. A melanoma *in situ* exhibiting a parallel ridge pattern (BRAAFF score = 3).

Dermoscopy has been shown to improve the discrimination between AM and acral naevi, mainly by highlighting two different patterns of pigment deposition, namely the PRP of melanoma and the PFP of naevi.[14–27] The latter are dermoscopically typified by the accentuation of the pigment along the furrows of the skin markings.[9,14,16,19,22–26] This pigmentation histopathologically corresponds to nests of melanocytes located around the crista profunda limitans, an epidermal rete ridge located under the surface furrows. In contrast, melanoma is typified by pigmentation along the ridges of the skin markings (Fig. 4), histopathologically corresponding to a proliferation of atypical melanocytes located mostly around the crista profunda intermedia.[15–18,21] These parallel line patterns are a result of the characteristic anatomy of the acral skin, and our results confirm their usefulness in the differentiation between AMs and acral naevi. However, our findings suggest that additional melanoma features should also be taken into consideration when evaluating an acral pigmented lesion, as a considerable proportion of AMs lack the PRP.

Analytically, in agreement with previous studies reporting 99% specificity of PRP, this criterion represented in our study the most potent predictor of melanoma, posing an 18-fold probability.[17] This means that the detection of PRP should warrant excision of the lesion, even in the absence of any other melanoma criteria and even if the lesion is characterized by perfect symmetry. However, PRPs were present in only 38·2% of AMs, meaning that > 60% of AMs might be overlooked if only PRP is considered (Figs 5, 6). This criterion was more common in melanoma *in situ* (50%) than in invasive AM (33%). The previously reported sensitivity of PRP as a single criterion for AM diagnosis has been reported to range

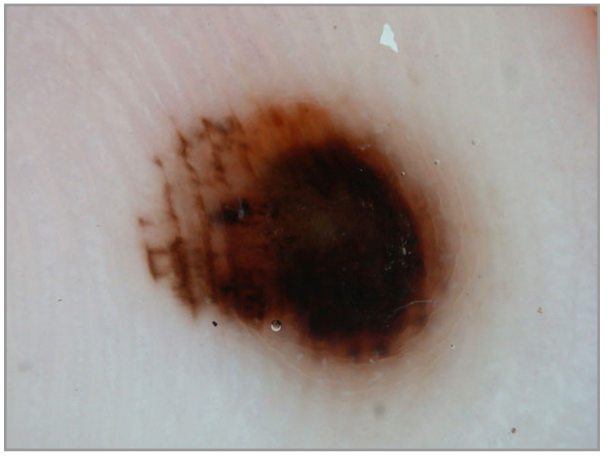

Fig 5. A 1·5-mm-thick melanoma displaying a parallel furrow pattern (−1 point), but also an irregular blotch (+1 point) and asymmetry of structures (+1 point), resulting in a BRAAFF score of 1.

Fig 6. A 1-mm-thick melanoma displaying an irregular blotch (BRAAFF score 1).

from 53% to 86%.[9,15,17,27] The lower frequency of PRP in our series might be related to the higher percentage of invasive tumours in our sample, as it is known that PRP is more common in early AM.

Similarly, although PFPs were the most potent predictor for the diagnosis of a naevus, posing a ninefold probability, 10% of AMs exhibited PFP in some parts of the lesion (Fig. 5). Subsequently, the detection of this feature should not exclude the diagnosis of AM when other melanoma-specific criteria are visualized. Similarly, a fibrillar pattern was associated with a threefold probability of a naevus, but they were also present in 7·6% of AMs. In line with our findings, the observation that 'benign' criteria might be focally present in AM has been highlighted recently by a collaborative study of the International Dermoscopy Society, which included mainly invasive AMs.[34]

Irregular diffuse pigmentation (IDP, also called blotches) has also been described as a common dermoscopic criterion of AM, and it has been suggested to typify mainly invasive tumours.[9,15,17,27] Phan *et al.* found IDP to represent the most common AM pattern in a series of AMs in Europe,[27] whereas in a recent multicentre study the frequency of IDP was significantly lower.[28] In our study, irregular blotches were found in 68·2% of melanomas, representing one of the most common criteria. A direct comparison between this number and the frequency of IDP in former studies is not possible, as we considered irregular blotches as a local feature and not as a global pattern as in the previously mentioned studies. However, our multivariate analysis revealed that irregular blotches are a potent melanoma predictor, imposing a fourfold increased probability of AM.

Asymmetry of colours and asymmetry of structures also represented potent melanoma predictors in our study, with a sevenfold and fourfold increased probability of AM, respectively. Notably, our data suggest that, in the presence of marked asymmetry (both in colours and structures), the lesion should be excised even in the presence of 'benign' criteria, such as PFP or fibrillar pattern.

The BRAAFF checklist allows a significant improvement of the diagnostic accuracy of dermoscopy for the diagnosis of AM, compared with any previously suggested method, with an acceptable cost in specificity. Of note, the subgroup analysis revealed that the BRAAFF checklist was valid for the detection of both *in situ* and invasive tumours. The higher sensitivity of the model for the diagnosis of invasive melanoma should be considered reasonable, as invasive tumours display, as a rule, more evident melanoma criteria. Furthermore, the accuracy of the BRAAFF checklist was high even when melanomas were compared only with excised naevi. This finding is particularly relevant for daily practice, as it highlights the power of this new model to discriminate melanoma from naevi that were previously judged suspicious enough to merit excision. However, despite the increased diagnostic accuracy of this model, some melanomas might still evade dermoscopic detection. Subsequently, it has to be underlined that the dermoscopic findings should always be interpreted within the clinical context of the patient, integrated with all relevant clinical information such as the patient's age and history, while histopathological examination is required in equivocal cases.

Dermoscopic algorithms (ABCD rule, 7-point checklist, Menzies method etc.) have been useful tools for guiding clinicians in everyday clinical practice.[35–37] The BRAAFF algorithm, by taking into consideration all of the dermoscopic criteria that are useful to differentiate acral naevi from AM, is a practical tool to help in the detection of AMs that deviate from the pathognomonic PRP, thus increasing the diagnostic accuracy. To simplify the interpretation of the algorithm further and to enhance its applicability, we provide below four simple management suggestions when examining an acral lesion. (i) A lesion dermoscopically exhibiting a PRP should be excised (Fig. 4); (ii) a lesion displaying a symmetric PFP or a symmetric fibrillar pattern is very probably benign and should not be excised; (iii) a lesion exhibiting a PFP or fibrillar pattern should be excised if displaying marked asymmetry (asymmetry of colours plus asymmetry of structures) or a

slight asymmetry (of colours or structures) plus irregular blotches (Fig. 5); and (iv) a lesion lacking a PRP, PFP or fibrillar pattern should be excised in the presence of asymmetry (of colours or structures or both) or in the presence of irregular blotches (Fig. 6).

Our study has several limitations. Firstly, the retrospective design is subject to recall and observational biases, which were addressed by involving three independent evaluators blinded to the clinical and histopathological diagnosis. Intraobserver agreement was moderate to substantial between investigators. For those variables where only a moderate agreement was achieved, this could be due to the low overall frequencies of these criteria in our dataset (see Table 2). Secondly, the histopathological diagnosis of acral melanocytic lesions might be highly problematic, as early melanoma might not display diagnostic criteria, while acral naevi might display criteria suggestive of melanoma (pseudomelanoma).[38] Furthermore, discrimination between *in situ* and invasive melanoma may also be problematic, as subtle features of microinvasion might be overlooked. Therefore, although we included only cases with a definite histopathological diagnosis on examination by expert dermatopathologists in the field, we cannot rule out the possibility that some tumours were misclassified. Thirdly, in the present study we included nonexcised naevi with a minimum follow-up of 1 year. Although unlikely, we cannot exclude the possibility that a lesion assessed as a naevus and remaining stable after 1 year is in fact a very slow-growing melanoma. Fourthly, we did not include cases of subcorneal haemorrhage in our study, which may also sometimes exhibit a PRP. Accordingly, the diagnostic accuracy to discriminate between AM and subcorneal haemorrhage remains to be elucidated further. Fifthly, we aimed to provide a purely dermoscopic algorithm, independently of clinical and epidemiological parameters. However, clinicians should take into consideration that the risk of melanoma increases with the patient's age, as shown by the results of the current and previous studies. Sixthly, the suggested algorithm was derived from a retrospective analysis of already diagnosed lesions and should be prospectively validated in future studies. Finally, considering the high morbidity of melanoma, we aimed for the highest possible sensitivity to ensure that the checklist provides early detection of the most possible AMs. For that, we included in the multivariate analyses more variables than recommended.[30] To overcome this limitation the proposed BRAAFF checklist requires external validation in future studies.

In conclusion, the BRAAFF checklist significantly improves the diagnostic accuracy of dermoscopy for the diagnosis of AM, compared with any previously suggested method, with an acceptable cost in specificity.

References

1 Ishihara K, Saida T, Otsuka F, Yamazaki N. The Prognosis and Statistical Investigation Committee of the Japanese Skin Cancer Society: statistical profiles of malignant melanoma and other skin cancers in Japan: 2007 update. *Int J Clin Oncol* 2008; **13**:33–41.

2 Seiji M, Takematsu H, Hosokawa M *et al.* Acral melanoma in Japan. *J Invest Dermatol* 1983; **80**:56s–60s.

3 Byrd KM, Wilson DC, Hoyler SS, Peck GL. Advanced presentation of melanoma in African Americans. *J Am Acad Dermatol* 2004; **50**:21–4.

4 Bellows CF, Belafsky P, Fortgang IS, Beech DJ. Melanoma in African-Americans: trends in biological behavior and clinical characteristics over two decades. *J Surg Oncol* 2001; **78**:10–16.

5 Cress RD, Holly EA. Incidence of cutaneous melanoma among non-Hispanic whites, Hispanics, Asians, and blacks: an analysis of California cancer registry data, 1988–93. *Cancer Causes Control* 1997; **8**:246–52.

6 Reintgen DS, McCarty KM Jr, Cox E, Seigler HF. Malignant melanoma in black American and white American populations: a comparative review. *JAMA* 1982; **248**:1856–9.

7 Stevens NG, Liff JM, Weiss NS. Plantar melanoma: is the incidence of melanoma of the sole of the foot really higher in blacks than whites? *Int J Cancer* 1990; **45**:691–3.

8 Saida T. Morphological and molecular uniqueness of acral melanoma. *Expert Rev Dermatol* 2007; **2**:125–31.

9 Saida T, Koga H, Uhara H. Key points in dermoscopic differentiation between early acral melanoma and acral nevus. *J Dermatol* 2011; **38**:25–34.

10 Bradford PT, Goldstein AM, McMaster ML, Tucker MA. Acral lentiginous melanoma: incidence and survival patterns in the United States, 1986–2005. *Arch Dermatol* 2009; **145**:427–34.

11 Green A, McCredie M, MacKie R *et al.* A case–control study of melanomas of the soles and palms (Australia and Scotland). *Cancer Causes Control* 1999; **10**:21–5.

12 Phan A, Touzet S, Dalle S *et al.* Acral lentiginous melanoma: a clinicoprognostic study of 126 cases. *Br J Dermatol* 2006; **155**:561–9.

13 Argenziano G, Ferrara G, Francione S *et al.* Dermoscopy – the ultimate tool for melanoma diagnosis. *Semin Cutan Med Surg* 2009; **28**:142–8.

14 Koga H, Saida T. Revised 3-step dermoscopic algorithm for the management of acral melanocytic lesions. *Arch Dermatol* 2011; **147**:741–3.

15 Oguchi S, Saida T, Koganehira Y *et al.* Characteristic epiluminescent microscopic features of early malignant melanoma on glabrous skin: a videomicroscopic study. *Arch Dermatol* 1998; **134**:563–8.

16 Saida T, Oguchi S, Miyazaki A. Dermoscopy for acral pigmented lesions. *Clin Dermatol* 2002; **20**:279–85.

17 Saida T, Miyazaki A, Oguchi S *et al.* Significance of dermoscopic patterns in detecting malignant melanoma on acral volar skin: results of a multicenter study in Japan. *Arch Dermatol* 2004; **140**:1233–8.

18 Saida T. Lessons learned from studies of the development of early melanoma. *Int J Clin Oncol* 2005; **10**:371–4.

19 Saida T, Oguchi S, Ishihara Y. *In vivo* observation of magnified features of pigmented lesions on volar skin using video macroscope. *Arch Dermatol* 1995; **131**:298–304.

20 Saida T. Malignant melanoma on the sole: how to detect the early lesions efficiently. *Pigment Cell Res* 2000; **13**:135–9.

21 Ishihara Y, Saida T, Miyazaki A *et al.* Early acral melanoma *in situ*: correlation between the parallel ridge pattern on dermoscopy and microscopic features. *Am J Dermatopathol* 2006; **28**:21–7.

22 Malvehy J, Puig S. Dermoscopic patterns of benign volar melanocytic lesions in patients with atypical mole syndrome. *Arch Dermatol* 2004; **140**:538–44.

23 Akasu R, Sugiyama H, Araki M *et al.* Dermatoscopic and videomicroscopic features of melanocytic plantar nevi. *Am J Dermatopathol* 1996; **18**:10–18.

24 Ozdemir F, Karaarslan IK, Akalin T. Variations in the dermoscopic features of acquired acral melanocytic nevi. *Arch Dermatol* 2007; **143**:1378–84.
25 Altamura D, Altobelli E, Micantonio T *et al*. Dermoscopic patterns of acral melanocytic nevi and melanomas in a white population in central Italy. *Arch Dermatol* 2006; **142**:1123–8.
26 Saida T, Koga H. Dermoscopic patterns of acral melanocytic nevi: their variations, changes, and significance. *Arch Dermatol* 2007; **143**:1423–6.
27 Phan A, Dalle S, Touzet S *et al*. Dermoscopic features of acral lentiginous melanoma in a large series of 110 cases in a white population. *Br J Dermatol* 2010; **162**:765–71.
28 Saida T, Koga H. Dermoscopy of pigmented lesions of the palms and soles. Available at: http://www.uptodate.com/contents/dermoscopy-of-pigmented-lesions-of-the-palms-and-soles (last acce ssed 15 July 2015).
29 Lallas A, Sgouros D, Zalaudek I *et al*. Palmar and plantar melanomas differ for sex prevalence and tumor thickness but not for dermoscopic patterns. *Melanoma Res* 2014; **24**:83–7.
30 Vittinghoff E, McCulloch CE. Relaxing the rule of ten events per variable in logistic and Cox regression. *Am J Epidemiol* 2007; **165**:710–18.
31 Steyerberg EW, Eijkemans MJC, Habbema JDF. Application of shrinkage techniques in logistic regression analysis: a case study. *Stat Neerl* 2001; **55**:76–88.
32 Conti EM, Cercato MC, Gatta G *et al*. Childhood melanoma in Europe since 1978: a population-based survival study. *Eur J Cancer* 2001; **37**:780–4.
33 Pappo AS. Melanoma in children and adolescents. *Eur J Cancer* 2003; **39**:2651–61.
34 Braun RP, Thomas L, Dusza SW *et al*. Dermoscopy of acral melanoma: a multicenter study on behalf of the international dermoscopy society. *Dermatology* 2013; **227**:373–80.
35 Stolz W, Riemann A, Cognetta AB. ABCD rule of dermatoscopy: a new practical method for early recognition of malignant melanoma. *Eur J Dermatol* 1994; **4**:521–7.
36 Argenziano G, Fabbrocini G, Carli P *et al*. Epiluminescence microscopy for the diagnosis of doubtful melanocytic skin lesions. Comparison of the ABCD rule of dermatoscopy and a new 7-point checklist based on pattern analysis. *Arch Dermatol* 1998; **134**:1563–70.
37 Menzies SW, Ingvar C, Crotty KA, McCarthy WH. Frequency and morphologic characteristics of invasive melanomas lacking specific surface microscopic features. *Arch Dermatol* 1996; **132**:1178–82.
38 Saida T, Kawachi S, Koga H. Anatomic transitions and the histopathologic features of melanocytic nevi. *Arch Dermatol* 2008; **144**:1232–3.

Supporting Information

Additional Supporting Information may be found in the online version of this article.

Table S1. Correlation Matrix of the multivariate model

Table S2. Backward elimination according to likelyhood criteria (full model of Table 4).

Table S3. Bootstrapped steps of Table S2 in arithmetic order.

Data S1. Additional analyses.